

SCIENTIFIC REPORTS

OPEN

Pharmacological profile and efficiency *in vivo* of diflapolin, the first dual inhibitor of 5-lipoxygenase-activating protein and soluble epoxide hydrolase

Ulrike Garscha¹, Erik Romp¹, Simona Pace¹, Antonietta Rossi², Veronika Temml³, Daniela Schuster³, Stefanie König¹, Jana Gerstmeier¹, Stefanie Liening¹, Markus Werner¹, Heiner Atze¹, Sandra Wittmann⁴, Christina Weinigel⁵, Silke Rummler⁵, Gerhard K. Scriba¹, Lidia Sautebin² & Oliver Werz¹

Arachidonic acid (AA) is metabolized to diverse bioactive lipid mediators. Whereas the 5-lipoxygenase-activating protein (FLAP) facilitates AA conversion by 5-lipoxygenase (5-LOX) to pro-inflammatory leukotrienes (LTs), the soluble epoxide hydrolase (sEH) degrades anti-inflammatory epoxyeicosatrienoic acids (EETs). Accordingly, dual FLAP/sEH inhibition might be advantageous drugs for intervention of inflammation. We present the *in vivo* pharmacological profile and efficiency of *N*-[4-(benzothiazol-2-ylmethoxy)-2-methylphenyl]-*N'*-(3,4-dichlorophenyl)urea (diflapolin) that dually targets FLAP and sEH. Diflapolin inhibited 5-LOX product formation in intact human monocytes and neutrophils with $IC_{50} = 30$ and 170 nM, respectively, and suppressed the activity of isolated sEH ($IC_{50} = 20$ nM). Characteristic for FLAP inhibitors, diflapolin (I) failed to inhibit isolated 5-LOX, (II) blocked 5-LOX product formation in HEK cells only when 5-LOX/FLAP was co-expressed, (III) lost potency in intact cells when exogenous AA was supplied, and (IV) prevented 5-LOX/FLAP complex assembly in leukocytes. Diflapolin showed target specificity, as other enzymes related to AA metabolism (i.e., COX1/2, 12/15-LOX, LTA₄H, LTC₄S, mPGES₁, and cPLA₂) were not inhibited. In the zymosan-induced mouse peritonitis model, diflapolin impaired vascular permeability, inhibited cysteinyl-LTs and LTB₄ formation, and suppressed neutrophil infiltration. Diflapolin is a highly active dual FLAP/sEH inhibitor *in vitro* and *in vivo* with target specificity to treat inflammation-related diseases.

The arachidonic acid (AA) cascade plays a central role in the biosynthesis of lipid mediators (LMs) with pro-inflammatory but also anti-inflammatory properties¹. In mammalian cells, AA is released from phospholipids by cytosolic phospholipase A₂ (cPLA₂) upon stimulation. Liberated AA can be converted via three different pathways to bioactive LMs: cyclooxygenases (COXs) catalyze the initial step in the formation of inflammation-initiating prostaglandins (PGs) and thromboxane (TX), whereas lipoxygenases (LOXs) form hydroperoxyeicosatetraenoic acids (HPETEs), leukotrienes (LTs), and lipoxins (LXs)². Moreover, AA is transformed by cytochrome P450 enzymes to monohydroxyeicosatetraenoic acids (HETEs) and epoxyeicosatrienoic acids (EETs)^{3,4}. EETs possess anti-inflammatory properties and are degraded by soluble epoxide hydrolase (sEH) to the corresponding diols (dihydroxyeicosatrienoic acids (DiHETrEs)) with associated loss of beneficial effects.

¹Chair of Pharmaceutical/Medicinal Chemistry, Institute of Pharmacy, Friedrich-Schiller-University Jena, Philosophenweg 14, D-07743, Jena, Germany. ²Department of Pharmacy, School of Medicine, University of Naples Federico II, 80131, Naples, Italy. ³Department of Pharmacy / Pharmaceutical Chemistry and Center for Molecular Biosciences Innsbruck (CMBI), University of Innsbruck, Innrain 80-82, A-6020, Innsbruck, Austria. ⁴Institute of Pharmaceutical Chemistry, Goethe University Frankfurt, 60438, Frankfurt, Germany. ⁵Institute of Transfusion Medicine, University Hospital Jena, 07743, Jena, Germany. Ulrike Garscha and Erik Romp contributed equally to this work. Correspondence and requests for materials should be addressed to U.G. (email: ulrike.garscha@uni-jena.de)

COX inhibitors that block PG and TX formation have been intensively studied and are widely used to treat pain and inflammation, albeit with frequent and severe side-effects⁵. Despite significant efforts in developing compounds that interfere with the other pathways of the AA cascade (e.g. 5-LOX), the respective candidates failed in clinical trials due to unpredicted side effects or lack of efficacy⁶. Targeting solely one pathway out of the AA cascade could be one reason for this issue⁷, which is well-known for shunting of AA towards the 5-LOX pathway due to inhibition of PG/TX formation by aspirin or other COX inhibitors⁸. Thus, compounds that selectively act on multiple targets (so-called designed multiple ligands – DML)^{9,10} may be appropriate to suppress the biosynthesis of pro-inflammatory LMs but maintain anti-inflammatory LMs. Such agents may be advantageous over single-interfering drugs and may represent a promising pharmacological approach for intervention with complex diseases as inflammation^{9,11–14}. We recently discovered ((*N*-[4-(benzothiazol-2-ylmethoxy)-2-methylphenyl]-*N'*-(3,4-dichlorophenyl)urea; compound 5 in ref. 15) as the first dual inhibitor of 5-lipoxygenase-activating protein (FLAP) and sEH by using a pharmacophore-based virtual screening¹⁵. This compound is now designated diflapolin. FLAP, a nuclear membrane integral protein^{16,17} assists 5-LOX in LT biosynthesis, and FLAP inhibitors (e.g. MK886, BAY-X 1005) efficiently abolish LT formation *in vitro* and *in vivo*^{18,19}. sEH degrades EETs with anti-inflammatory and antihypertensive properties to DiHETrEs that are assumed to be pro-inflammatory with additional detrimental properties²⁰. Therefore, sEH inhibition is not only elevating EET levels, it rather stabilizes epoxy-fatty acids with favorable actions. It was recently reported that co-administration of a sEH inhibitor with a FLAP inhibitor enhanced the anti-inflammatory activities in a murine model²¹, whereas sole inhibition of sEH lead to albuminuria²². These data support the development of dual FLAP/sEH inhibitors to achieve better therapeutic effects due to simultaneous suppression of pro-inflammatory LTs and DiHETrEs but maintaining anti-inflammatory EETs. Here, we present the molecular pharmacological profile and the effectiveness of the first dual FLAP/sEH inhibitor diflapolin¹⁵ using cell-free and cell-based analysis of biosynthetic pathways of the AA cascade as well as animal models of inflammation. We find that diflapolin is target-specific for sEH and FLAP with strong potencies and represents a highly effective anti-inflammatory compound.

Results

Diflapolin inhibits cellular 5-LOX product formation without affecting 5-LOX in cell-free assays.

Based on a pharmacophore-based virtual screening campaign, diflapolin was identified as most potent agent out of 20 hit compounds that dually inhibited FLAP and sEH in simple screening assays¹⁵. The structure of diflapolin is composed of a urea moiety (present in the sEH reference inhibitor AUDA) potentially binding to sEH as a mimetic of epoxides, and an aromatic heterocyclic scaffold (benzothiazole, seemingly reflecting the indole scaffold of the reference FLAP inhibitor MK886) that may primarily confer FLAP interference (Fig. 1a). We first aimed to investigate the interference of diflapolin with FLAP and thus with 5-LOX product biosynthesis in more detail. Since FLAP does apparently not possess any measurable enzyme activity that can be readily monitored in a cell-free assay, functional interference of a given compound with FLAP requires indirect analysis of 5-LOX activation and product formation in intact cells²³. In intact monocytes and neutrophils from human peripheral blood stimulated with Ca²⁺-ionophore, diflapolin effectively inhibited the formation of LTB₄ and its isomers and of 5-H(p)ETE with IC₅₀ values of 30 and 170 nM, respectively (Fig. 1b). In order to exclude direct inhibition of 5-LOX, diflapolin was analyzed against 5-LOX activity in cell-free assays. Diflapolin, up to 10 μM, did not significantly inhibit the activity of isolated human recombinant 5-LOX (not shown) or of 5-LOX in homogenates of neutrophils and monocytes (Fig. 1b). The same pattern of interference with 5-LOX product formation was observed for the FLAP inhibitor MK886 (IC₅₀ monocytes: ~3 nM, neutrophils: 10–14 nM; IC₅₀ 5-LOX in cell-free assays: >10 μM, not shown), which is in agreement with the literature²⁴. In contrast, the direct 5-LOX inhibitor zileuton inhibited 5-LOX activity in the cell-based (monocytes, neutrophils) and cell-free assays about equally well (IC₅₀ = 1.5 and 0.8 μM, respectively), as reported²⁵. A typical feature of FLAP inhibitors is their loss of efficiency, when cells are stimulated for 5-LOX product formation in the presence of exogenous AA, since (I) FLAP inhibitors compete with AA binding within the active site of FLAP²⁶, and (II) ample AA supply may circumvent the requirement of FLAP for cellular 5-LOX product formation^{27,28}. In both monocytes and neutrophils, increasing levels of AA (up to 60 μM) sequentially reduced the inhibitory potency of diflapolin and shifted the IC₅₀ values from 30 and 170 nM, respectively, (no AA supplementation) to >10 μM (at 60 μM AA) (Fig. 1c/d). These data suggest that diflapolin binds in the fatty acid substrate (AA) pocket of FLAP.

To confirm the hypothesis that diflapolin acts as FLAP inhibitor, we studied suppression of 5-LOX product formation in stably transfected HEK293 cells that either express 5-LOX plus FLAP or 5-LOX alone. Note that induction of 5-LOX product formation in HEK293 cells requires supplementation of exogenous AA (regardless of FLAP)²⁹ and we therefore stimulated the cells with A23187 plus 3 μM AA. Diflapolin strongly inhibited 5-LOX product formation in intact HEK293 cells expressing both 5-LOX and FLAP, whereas in HEK293 cells deficient in FLAP, 5-LOX product formation was hardly impaired by diflapolin (Fig. 1e). Together, these data show that diflapolin inhibits 5-LOX product formation only when FLAP is operative supporting FLAP as target of diflapolin.

Diflapolin inhibits epoxide hydrolase activity of sEH without affecting the phosphatase activity.

sEH is a bifunctional enzyme with a C-terminal epoxide hydrolase (EH) and an N-terminal phosphatase activity that operate independent from each other³⁰. In a cell-free assay, diflapolin reduced the EH activity of human recombinant sEH with an IC₅₀ of 20 nM (Fig. 2a), comparable to the activity of AUDA (IC₅₀ = 69 nM), a well-recognized reference inhibitor of sEH³¹. sEH is constitutively expressed in the human liver cancer cell line HepG2 making it suitable as cell-based test system for evaluation of diflapolin for sEH inhibition in the cellular context. HepG2 cells were pre-treated with diflapolin and control inhibitors, and incubated with the sEH substrate 14,15-EET. sEH activity was then analyzed by monitoring 14,15-DiHETrE formation using UPLC-MS/MS. Diflapolin as well as AUDA inhibited cellular sEH activity to ~50% at 1 μM (Fig. 2b). Further decrease at concentrations up to 10 μM could not be observed, probably due to EET degradation that was sEH-independent and

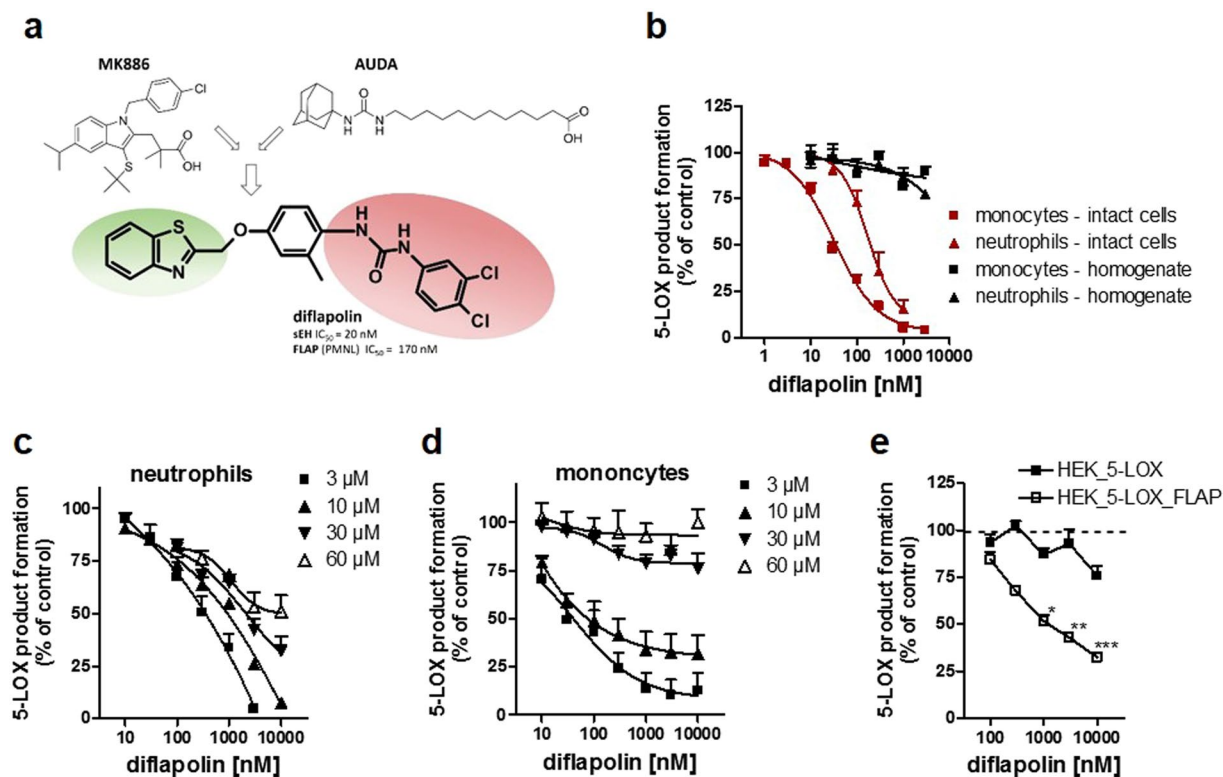


Figure 1. Diflapolin inhibits cellular 5-LOX product formation by targeting FLAP. (a) Chemical structure of the dual FLAP/sEH inhibitor diflapolin, with potential pharmacophoric moieties of typical FLAP (MK886) and sEH (AUDA) inhibitors. (b) Inhibition of 5-LOX product formation in human monocytes and neutrophils and in corresponding cell homogenates. Cells were pre-incubated with diflapolin (or 0.1% DMSO as vehicle) for 15 min and stimulated with 2.5 μ M Ca^{2+} -ionophore A23187 for 10 min. Cell homogenates were pre-incubated with diflapolin (or 0.1% DMSO) for 10 min at 4 $^{\circ}$ C, pre-warmed at 37 $^{\circ}$ C for 30 sec, and 20 μ M AA plus 1 mM $CaCl_2$ was added for another 10 min at 37 $^{\circ}$ C. 5-LOX products were analyzed by HPLC. (c,d) Effects of exogenous AA on the potency of diflapolin for inhibition of 5-LOX product formation in neutrophils (c) and monocytes (d). Cells were pre-treated by diflapolin (or 0.1% DMSO as vehicle) at 37 $^{\circ}$ C for 15 min, and subsequently activated by 2.5 μ M Ca^{2+} -ionophore A23187 plus the indicated concentrations of exogenous AA for another 10 min. (e) HEK293 cells expressing 5-LOX or 5-LOX and FLAP were pre-incubated with diflapolin and stimulated with 5 μ M Ca^{2+} -ionophore A23187 plus 3 μ M AA for 10 min at 37 $^{\circ}$ C. 5-LOX products were analyzed by HPLC. Data, expressed as percentage of vehicle control (=100%), are given as means \pm S.E.M, n = 3 *p < 0.05; **p < 0.005; ***p < 0.001 vs. vehicle control (ANOVA + Bonferroni with logarithmized values).

potentially non-enzymatic, as recombinant sEH in the corresponding cell-free assay yielded comparable results (Fig. 2b). AUDA reduced the sEH activity in a comparable manner, whereas MK886 and SC57461A (LTA₄-H inhibitor) had no impact on sEH in the cell-based sEH assay (Fig. 2c).

Next, we tested diflapolin against the phosphatase activity of sEH in a cell-free assay. Of interest, diflapolin failed to inhibit the phosphatase activity even at high concentrations (10 μ M) (Fig. 2d). In order to demonstrate that diflapolin as a specific inhibitor of the hydrolase activity of sEH, its effect on LTA₄-H was determined. LTA₄-H hydrolyses the epoxide in LTA₄ that is produced from AA by 5-LOX in a co-incubation experiment using isolated 5-LOX and LTA₄-H, where LTB₄ is formed. Diflapolin failed to inhibit LTA₄-H activity (i.e. LTB₄ formation) up to 10 μ M, compared to the LTA₄-H inhibitor SC57461A (IC_{50} of 0.1 μ M against recombinant LTA₄-H)³² that blocked LTB₄ biosynthesis and shifted the conversion of LTA₄ towards the non-enzymatically formed trans-isomers of LTB₄ (Fig. 2e). AUDA (10 μ M) showed the same pattern as diflapolin, whereas zileuton (3 μ M) as a direct 5-LOX inhibitor reduced the formation of all LTB₄ isomers (Fig. 2e), as expected due to reduced LTA₄ formation.

Effects of diflapolin on other eicosanoid biosynthetic enzymes. We next investigated the impact of diflapolin on other enzymes within the AA cascade that are involved in the biosynthesis of various eicosanoids in addition to FLAP and sEH. Besides FLAP, the LTC₄S and mPGES-1 belong to the membrane-associated proteins in eicosanoid and glutathione metabolism (MAPEG) family sharing high sequence and structure homology to FLAP^{33,34}. Potent FLAP inhibitors (like MK886 or BRP-187) inhibit the MAPEG family members LTC₄S and mPGES-1 as well^{27,35,36}. In contrast, diflapolin failed to inhibit LTC₄S and mPGES-1 activity in cell-free assays up to 10 μ M (Fig. 3a,b), which indicates a high target specificity of diflapolin among the MAPEGs. Also, diflapolin did not significantly inhibit the activities of COX-1 and -2 in cell-free assays (Fig. 3c), whereas the reference drug indomethacin blocked COX activities, as expected. The activities of other LOXs (i.e. 12-LOX and 15-LOX) in neutrophils incubated with A23187 and 20 μ M AA were not inhibited by diflapolin. In contrast, 15-HETE formation

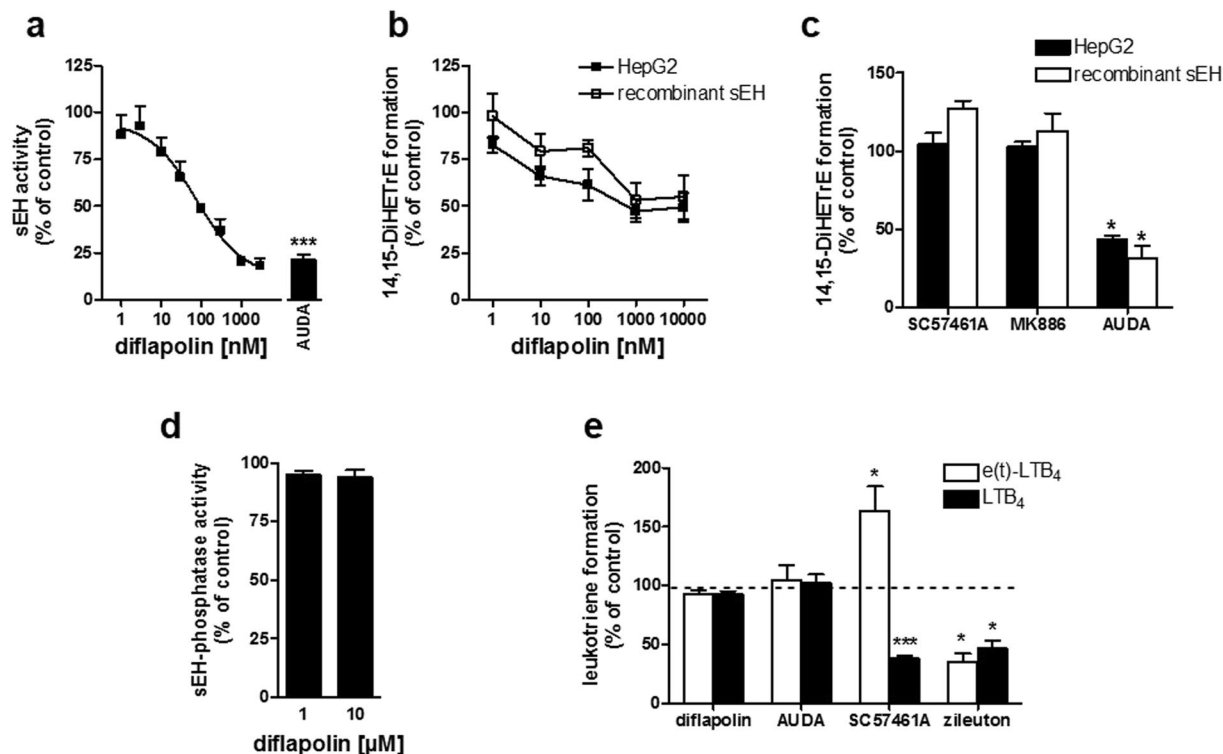


Figure 2. Diflapolin inhibits epoxide hydrolase activity of sEH. **(a)** The epoxide hydrolase activity of human recombinant sEH was analyzed in fluorescence-based cell-free assay. Diflapolin, AUDA (300 nM), or DMSO (vehicle, 0.1%) was added to sEH and after 10 min at 4 °C, the reaction was started by addition of the substrate (50 µM PHOME) and stopped after 60 min before analyzing the fluorescent product. Data are expressed in percentage of control and are given as means \pm S.E.M., $n = 3-4$, *** $p < 0.001$; vs vehicle (paired t-test). **(b/c)** sEH activity was analyzed in intact HepG2 cells and for recombinant sEH. Cells and enzyme were pre-incubated with DMSO (vehicle, 0.1%), diflapolin (indicated concentrations), SC57461A (0.3 µM), AUDA (5 µM) or MK886 (0.3 µM), and then incubated with 14,15-EET. Amounts of 14,15-EET and 14,15-DiHETE were analyzed by UPLC-MS/MS. Data are expressed as percentage of control and are given as means \pm S.E.M., $n = 3$, * $p < 0.05$; versus vehicle (paired t-test). **(d)** Phosphatase activity of sEH was analyzed in a fluorescence-based cell-free assay. Diflapolin or DMSO (vehicle, 0.1%) was added to human recombinant phosphatase domain of sEH for 10 min at 4 °C, the reaction was initiated by addition of DiFMUP (300 µM) and fluorescence was analyzed for 45 min. Data are expressed as percentage of vehicle control (100%), are given as means \pm S.E.M., $n = 3$ * $p < 0.05$ vs. vehicle control (paired t-test). **(e)** Co-incubations of human recombinant 5-LOX and LTA₄-H in PBS plus 1 mM EDTA pre-incubated with diflapolin (10 µM), AUDA (10 µM), SC57461A (0.3 µM), zileuton (3 µM), or vehicle (0.1% DMSO) for 10 min on ice and subsequently stimulated by 20 µM AA and CaCl₂ for 10 min at 37 °C. LTB₄ isomers were analyzed by HPLC. Data are expressed as percentage of vehicle control (100%), are given as means \pm S.E.M., $n = 3-4$. * $p < 0.05$ vs. vehicle control (paired t-test with logarithmized values).

was concentration-dependently elevated (up to 200% of the vehicle control) (Fig. 3d). Since diflapolin was most potent in leukocytes to suppress 5-LOX product formation from endogenous AA but ineffective when high concentrations of exogenous AA were supplied, the compound could act at the level of AA release. However, in [³H] AA-pre-labelled neutrophils, diflapolin even at high concentrations (1 µM) did not inhibit the release of AA upon A23187-stimulation, as compared to the cPLA₂ inhibitor RSC-3388 that suppressed AA liberation (Fig. 3e). Finally, detrimental effects on cellular viability could be excluded, as diflapolin (10 µM) did not affect the viability of monocytes in a MTT assay at 24 or 48 hrs, while staurosporine (3 µM, positive control) strongly impaired cell viability under these conditions (Fig. 3f). Taken together, diflapolin dually and strongly inhibits FLAP and sEH with target specificity as it did not interfere with other AA pathway-related enzymes (LTA₄-H, COX-1/2, cPLA₂, 12/15-LOXs) and FLAP-related MAPEG enzymes such as mPGES₁ and LTC₄S.

Effects of diflapolin on 5-LOX subcellular redistribution and 5-LOX/FLAP complex assembly. 5-LOX, a soluble cytosolic or intranuclear enzyme in resting leukocytes, translocates to the nuclear envelope upon cell activation and co-localizes with FLAP at the nuclear membrane to form a tight LT biosynthetic complex^{37, 38}. Immunofluorescence microscopy studies using human neutrophils or monocytes showed that neither diflapolin nor the FLAP inhibitor MK886 or the 5-LOX inhibitor zileuton prevented co-localization of 5-LOX with FLAP (Fig. 4). However, diflapolin efficiently prevented the tight 5-LOX/FLAP complex assembly,

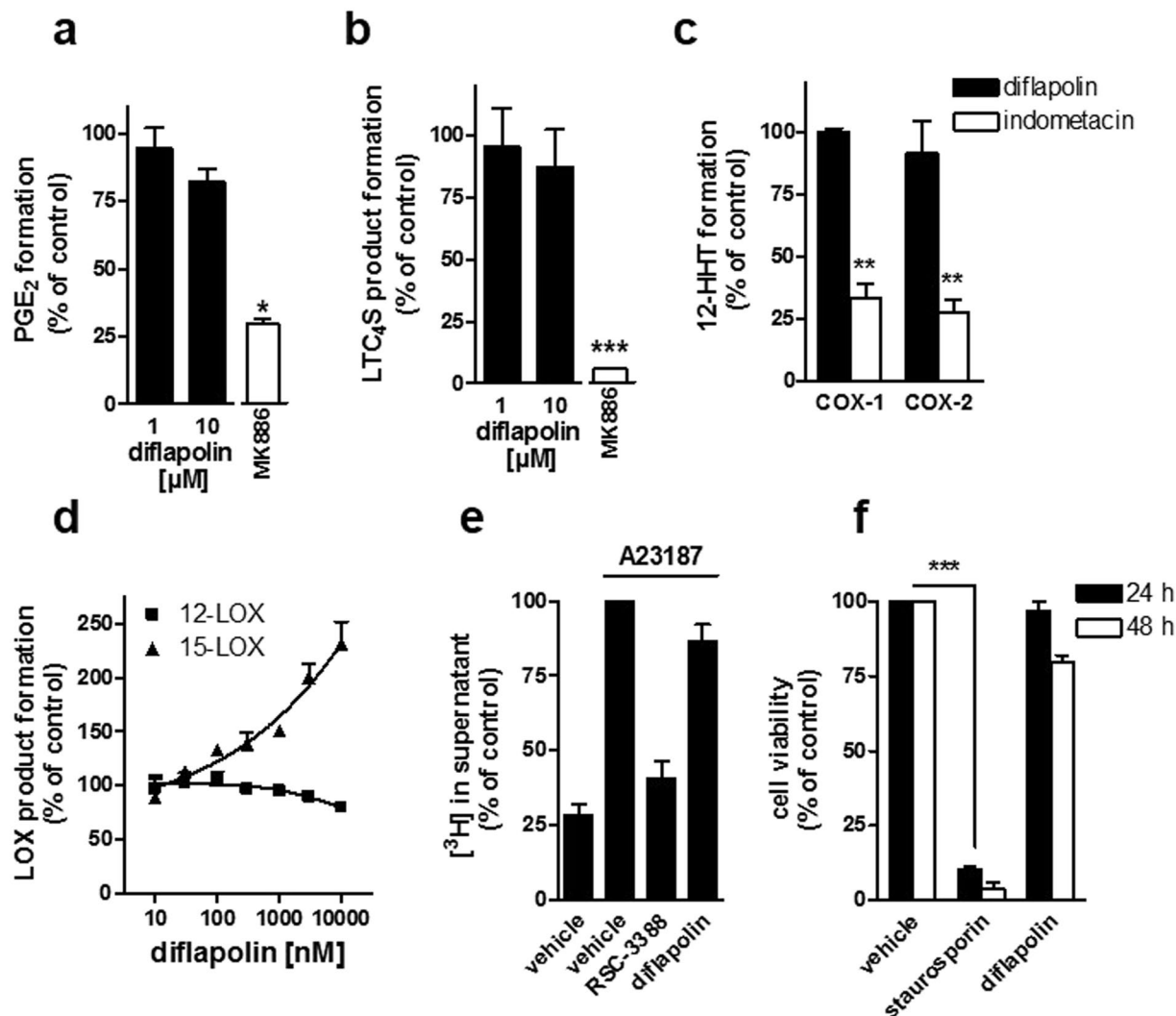


Figure 3. DiFlapolin shows target specificity within the AA cascade without cytotoxicity. **(a)** mPGES-1 activity. Microsomes of IL-1 β -stimulated A549 cells were pretreated with diFlapolin, 10 μ M MK886, or vehicle for 10 min on ice and stimulated with 20 μ M PGH₂. After 1 min at 4 $^{\circ}$ C, PGE₂ formation was analyzed by HPLC. **(b)** LTC₄S activity. Microsomes of LTC₄S-expressing HEK293 cells were pretreated with diFlapolin, MK886 (10 μ M), or vehicle for 10 min on ice with subsequent addition of LTA₄-methyl ester. After 10 min at 4 $^{\circ}$ C, LTC₄-methyl ester was analyzed by UPLC-MS/MS. **(c)** COX-1/2 activity. In cell-free assays, purified ovine COX-1 and recombinant human COX-2 were pretreated with diFlapolin (10 μ M), indometacin (10 μ M) or vehicle (0.1% DMSO) for 5 min on ice and stimulated with AA (5 and 2 μ M for COX-1 and -2, respectively) for 10 min at 37 $^{\circ}$ C. 12-HHT was analyzed by HPLC. **(d)** Effect of diFlapolin on 12- and 15-LOX. Intact neutrophils were preincubated by diFlapolin or vehicle (0.1% DMSO) and stimulated with 2.5 μ M Ca²⁺-ionophore plus 20 μ M AA for 10 min at 37 $^{\circ}$ C. 12- and 15-HETE were determined by HPLC. **(e)** AA release. [³H]AA-labeled neutrophils were pretreated with diFlapolin (1 μ M), RSC-3388 (10 μ M) or vehicle (0.1% DMSO) and stimulated by 2.5 μ M Ca²⁺-ionophore for 15 min. Radioactivity of the supernatant was analyzed by scintillation counting. **(f)** Cell viability assay. Monocytes were treated with diFlapolin (10 μ M), staurosporin (3 μ M) or vehicle (0.3% DMSO) for 24 and 48 h, respectively. Cell viability was determined by MTT assay. Data are expressed as percentage of control (100%), means \pm SEM, n = 3–5. *p < 0.05; **p < 0.005; ***p < 0.001 vs. vehicle control (paired t-test).

visualized by proximity-ligation assay (PLA) (Fig. 4), a common feature of FLAP inhibitors³⁷. MK886 gave comparable effects, whereas the 5-LOX inhibitor zileuton failed in this respect.

DiFlapolin exhibits potent anti-inflammatory properties in *in-vivo* experiments. We next investigated the anti-inflammatory effectiveness of diFlapolin in the zymosan-induced peritonitis mouse model³⁹ that is strongly related to the pathophysiological activities of LTs. DiFlapolin pre-treatment (1, 3 and 10 mg/kg, i.p. 30 min before zymosan injection) induced a significant reduction of LTC₄ and LTB₄ peritoneal levels, starting from the dose of 1 mg/kg (Fig. 5a and b) and comparable to the effect of MK886 (1 mg/kg, i.p. 30 min before zymosan). Since LTB₄ is a major chemoattractant for leukocytes, diFlapolin and MK886 caused concomitant block of leukocyte recruitment, which was dose-dependent for diFlapolin (Fig. 5c). Accordingly, at the dose of 10 mg/kg,

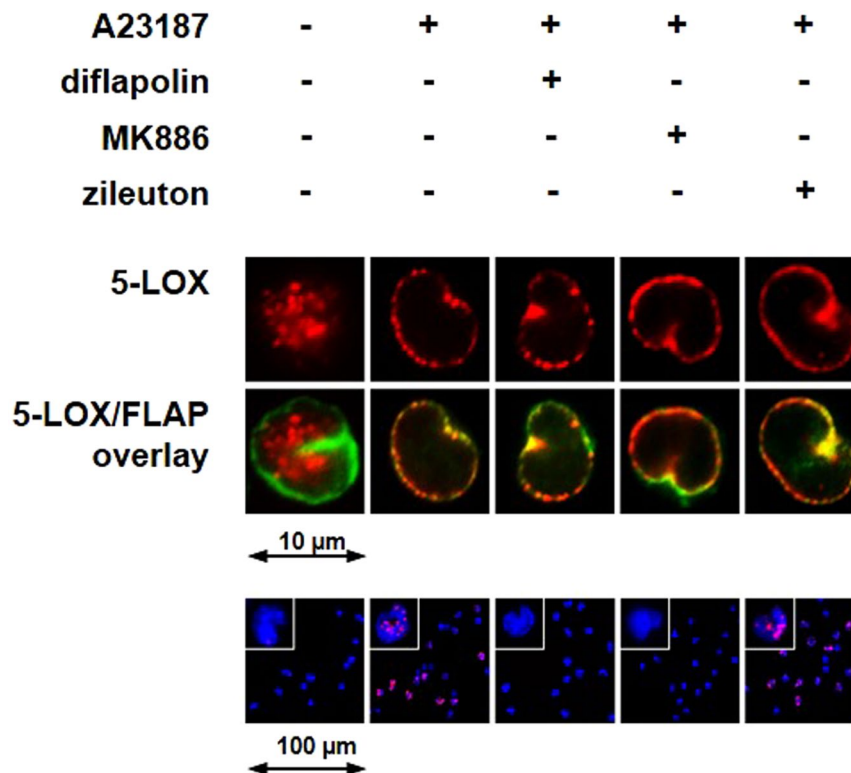


Figure 4. Effect of diflapolin on 5-LOX subcellular redistribution and 5-LOX/FLAP interaction. Cells were pretreated with diflapolin (1 μ M), MK886 (0.3 μ M), zileuton (3 μ M) or 0.1% DMSO for 15 min, and then stimulated with 2.5 μ M Ca^{2+} -ionophore A23187 for 10 min at 37 $^{\circ}$ C. Top panel: immunofluorescence microscopy was used to determine 5-LOX subcellular localization. Single images (top lane) show 5-LOX staining (red) and the overlay of 5-LOX (red) and FLAP (green) (middle lane). Results are representative for 100 individual cells of three independent experiments. Lower panel: *in situ* PLA was applied to determine 5-LOX/FLAP complex assembly in monocytes (lower panel) using antibodies against 5-LOX and FLAP. DAPI stains the nucleus (blue), and PLA signals by 5-LOX/FLAP complexes are stained in magenta. Results are representative for 100 individual cells of three independent experiments.

diflapolin inhibited the activity of MPO, a typical marker protein for neutrophils to $52.8 \pm 12.2\%$ (mean \pm SEM) vs. vehicle control and reduced vascular permeability to $55.7 \pm 14.4\%$ (mean \pm SEM) vs. vehicle control (Table 1), compared to inhibitory effects of MK886 (1 and 3 mg/kg) to $58.5 \pm 10.6\%$ and $48.6 \pm 3.2\%$, respectively.

Discussion

Our recent pharmacophore-based virtual screening campaign for dual FLAP/sEH inhibitors proposed diflapolin as most promising hit and novel chemotype targeting both FLAP and sEH¹⁵. Here, we disclose diflapolin as a potent, dual inhibitor of FLAP and sEH with marked anti-inflammatory efficacy *in vivo* and high target selectivity. Side-by-side studies of diflapolin with the “FLAP benchmark inhibitor” MK886⁴⁰ revealed comparable potencies for inhibition of 5-LOX product biosynthesis in human leukocytes *in vitro*, and about equal effectiveness in suppression of LT formation and inflammatory properties *in vivo* using murine zymosan-induced peritonitis models.

The identification of novel chemotypes as FLAP inhibitors is hampered due to the lack of distinct assays that unequivocally proof direct and functional interference of a given compound with FLAP²³. Thus far, no enzymatic activity has been assigned to FLAP that can be exploited as read-out in FLAP inhibitor discovery approaches. Moreover, FLAP does not support 5-LOX activity in cell-free assays (e.g. homogenates)⁴¹. Nevertheless, FLAP is essential for LT biosynthesis in intact cells and *in vivo*, as reflected by results from various pharmacological approaches⁴⁰ and from gene intervention using FLAP knock-out mice⁴². Experimental evidence suggests that FLAP operates as a 5-LOX helper protein for transforming AA to 5-HPETE and for dehydration of 5-HPETE to LTA₄^{29,43}. FLAP is able to bind AA²⁶ and to stimulate conversion of AA and 5-HPETE by 5-LOX⁴⁴, and along these lines AA or 5-HPETE were required for *in situ* 5-LOX/FLAP complex assembly at the nuclear membrane in activated cells^{37,38}. Together, it appears that FLAP binds released AA and/or *de novo*-formed 5-HPETE and transfers them to 5-LOX, thus permitting optimal access of 5-LOX towards its substrates.

In light of these facts, assignment of a small molecule as FLAP inhibitor requires certain characteristics, which are all fulfilled by diflapolin. First of all, diflapolin did not randomly emerge as 5-LOX product biosynthesis inhibitor but was identified in a target-directed screening campaign for dual FLAP/sEH inhibitors applying two independently created ligand-based pharmacophore models¹⁵. Second, diflapolin potently inhibited LT biosynthesis

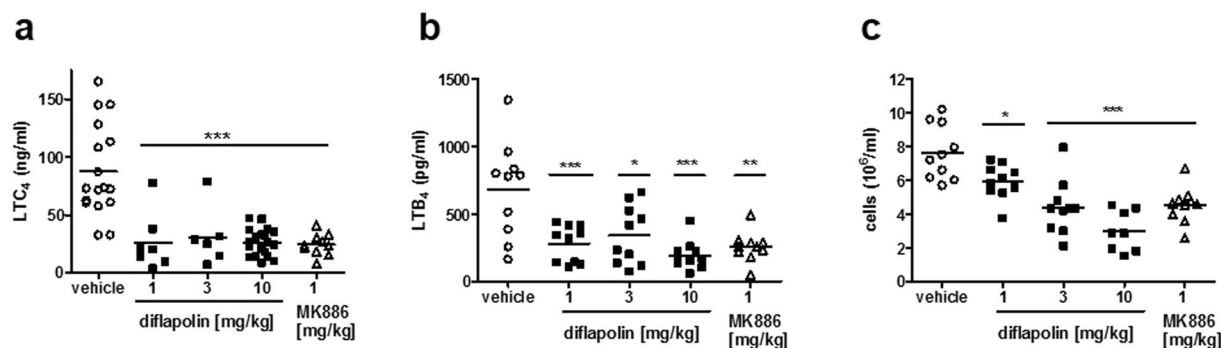


Figure 5. Effect of diflapolin on LTC_4 and LTB_4 formation, and cell recruitment in zymosan-induced peritonitis. Male mice ($n = 6-19$, each group) were treated i.p. with diflapolin, MK886 or vehicle, 30 min before induction of zymosan-induced peritonitis. (a) LTC_4 levels were analysed 30 min after zymosan injection by ELISA. (b) LTB_4 formation and (c) cell infiltration were analysed 4 h after zymosan injection. * $p < 0.05$; ** $p < 0.01$, *** $p < 0.001$ versus vehicle (Anova + Bonferroni).

	vascular permeability		myeloperoxidase activity	
	absorption (610 nm)	% of vehicle control	U/mL	% of vehicle control
vehicle	0.623 ± 0.04	100	1.23 ± 0.13	100
diflapolin 10 mg/kg	0.347 ± 0.09	55.7 ± 14.4	0.65 ± 0.15	52.8 ± 12.2
MK886 1 mg/kg	n.d.	n.d.	0.72 ± 0.13	58.5 ± 10.6
MK886 3 mg/kg	0.303 ± 0.02	48.6 ± 3.2	n.d.	n.d.

Table 1. Effect of diflapolin on vascular permeability and myeloperoxidase (MPO) activity in zymosan-induced peritonitis. Male mice ($n = 5$ for vascular permeability, $n = 7$ for MPO; each group) were treated i.p. with diflapolin, MK886, or vehicle, 30 min before induction of zymosan-induced peritonitis. Analysis of vascular permeability and MPO was performed 30 min and 4 h, respectively, after zymosan injection. Data are given means ± S.E.M, (vascular permeability $n = 5$; myeloperoxidase activity $n = 7$) * $p < 0.05$ versus vehicle (Anova + Bonferroni). n.d., not determined.

only in intact leukocytes (without being cytotoxic or suppressing AA substrate release) but did not directly affect the activity of isolated human recombinant 5-LOX or 5-LOX in leukocyte homogenates. Third, ample supply of exogenous AA strongly reduced the potency of diflapolin in stimulated neutrophils and monocytes, compatible with the proposed competition between AA and FLAP inhibitors for binding to FLAP⁴³. Fourth, diflapolin prevented the agonist-induced 5-LOX/FLAP complex assembly at the nuclear membrane in monocytes, visualized by PLA^{27,37}, without blocking 5-LOX translocation to the nucleus. Finally, the most striking proof for diflapolin inhibiting 5-LOX product formation by acting on FLAP but not on 5-LOX, is deduced from the fact that diflapolin suppresses cellular 5-LOX activity in 5-LOX-transfected HEK293 cells only when FLAP was co-expressed, while in cells devoid of FLAP, diflapolin failed in this respect. Note that these features of diflapolin were shared also with the FLAP inhibitor MK886 but not with the direct 5-LOX inhibitor zileuton (refs 27, 29, 37, 41 and 45 and this study). In conclusion, diflapolin is a potent LT biosynthesis inhibitor that confers its activity via inhibition of FLAP.

Besides FLAP, diflapolin was identified as potential hit using pharmacophore models for sEH inhibitors¹⁵, and it potently inhibited the epoxide hydrolase activity of sEH in a cell-free assay (IC_{50} 20 nM), while the phosphatase activity was not affected. In contrast, the epoxide hydrolase activity of $\text{LTA}_4\text{-H}$ was not affected by diflapolin, indicating specificity for sEH. Interference of diflapolin with sEH is not surprising since the urea moiety is a typical structural feature of sEH inhibitors that prevent the degradation of EETs^{12,46}. EETs formed from AA by CYP enzymes display anti-inflammatory and antihypertensive properties, maintain vascular homeostasis, and act generally cardio-protective^{20,47}. Among several EET degrading pathways, sEH metabolizes EETs to the corresponding dihydroxyeicosatrienoic acids (DiHETrE) with accompanied loss of health-promoting benefits^{20,48}. Accordingly, inhibition of sEH elevates EET levels leading to various beneficial effects. Little is known about the physiological role of the phosphatase activity, but an influence on the regulation of the endothelial nitric oxide synthase (eNOS) and NO-mediated effect on endothelial cells was suggested⁴⁹.

Because FLAP is a member of the MAPEG family, other structurally-related MAPEG members such as mPGES-1 and LTC_4S might be targeted by diflapolin as well, which is the case for the FLAP inhibitors MK866^{36,50} and BRP-187²⁷ that interfere with all three of these proteins. Diflapolin had no impact on mPGES-1 and LTC_4S activity up to 10 μM , suggesting target specificity within the MAPEG family. Moreover, other enzymes within the

AA cascade including COX-1/2, epoxide hydrolase activity of LTA₄-H, 12-LOX and 15-LOXs were not inhibited by diflupolol. Interestingly, formation of 15-HETE in neutrophil incubations was concentration-dependently increased by diflupolol, which might be explained by AA shunting towards the 15-LOX pathway. This may promote the formation of anti-inflammatory and pro-resolving LMs such as lipoxins, resolvins and protectins⁵¹. A shift from biosynthesis of pro-inflammatory eicosanoids and other oxylipins towards anti-inflammatory and pro-resolving LMs would certainly strengthen the power of dual FLAP/sEH inhibitors. Additionally, even though comprehensive data are yet not available, it is reasonable to assume that epoxy-fatty acids derived from other polyunsaturated fatty acids confer anti-inflammatory properties.

The current development of LT biosynthesis inhibitors as therapeutics focusses on FLAP inhibitors²³. Early representatives such as the indole MK886¹⁸ and the quinoline BAY X-1005¹⁹ are highly effective *in vitro* but probably due to their high lipophilicity they suffered from strong plasma protein binding, competition with fatty acids and, as a consequence reduced activity *in vivo*^{17,40}. However, more advanced compounds including the MK886 follow-up GSK2190915, the tetrahydrofuran derivative AZD6642 and the oxadiazole-based BI665915 are less prone to plasma protein binding with advantageous pharmacokinetics²³. These compounds are under active development (some entered clinical trials), and they appear to have lower risks of side effects as compared to 5-LOX inhibitors⁴⁰. Diflupolol is structurally unrelated to these above-mentioned chemotypes and represents the first FLAP inhibitor with a polar urea moiety (seemingly the pharmacophore for sEH interference) and high efficiency *in vivo*.

In order to evaluate the *in vivo* efficacy and anti-inflammatory potential of diflupolol, we utilized the zymosan-induced peritonitis mouse model that is well established as test system for studying LT biosynthesis *in vivo*³⁹. Our data show that diflupolol is about equally effective as MK886 in reducing LTB₄ and LTC₄ levels in the peritoneal exudates with consequent biological functions. LTB₄ is a potent chemotactic agent for neutrophils⁵² and in fact, neutrophil infiltration into the peritoneal cavity was strongly reduced by diflupolol. Cys-LTs mediate plasma extravasation⁵³ and diflupolol significantly impaired vascular permeability during peritonitis. Conclusively, diflupolol potently inhibits LT formation *in vivo* connected with anti-inflammatory activity.

We speculate that dual inhibition of FLAP and sEH inhibitor may have synergistic anti-inflammatory and cardio-protective actions. Indeed, increased levels of EETs seem to be cardio-protective⁴⁷ and FLAP was reported to be linked to certain cardiovascular diseases⁵⁴. DMLs that block sEH and COX or sEH and 5-LOX are proposed to have improved anti-inflammatory activities over compounds that interfere with only one target enzyme^{12,13,21,55}. Such DMLs dually targeting sEH and FLAP are thus far unknown. Future studies addressing the pharmacological relevance of suppression of LTs with accompanied elevation of EETs may reveal potential benefit in the therapy of inflammatory and cardiovascular diseases.

Taken together, here we provide substantial evidence that diflupolol acts as potent dual FLAP/sEH inhibitor with high target specificity. The compound lacks acute cytotoxicity and efficiently suppresses LT biosynthesis *in vivo* connected with potent anti-inflammatory activity in a mouse model. Based on these features, diflupolol might be a valuable chemical tool for studying the biology of FLAP and sEH, particularly as synergizing targets, and may represent a useful lead for evaluation of the therapeutic potential of dual FLAP and sEH inhibition in inflammatory and cardiovascular disorders.

Materials and Methods

Materials. Diflupolol was obtained from Specs designated AQ-090/41740539 (Zoetermeer, Netherlands). Bovine serum albumin (BSA), EDTA, glutathione, saccharose, and Tris, AppliChem (Darmstadt, Germany); L-glutamine, BioChem GmbH (Karlsruhe, Germany); β-PGE₂ and tritium-labeled [5,6,8,9,11,12,14,15-³H] labeled AA, Biotrend Chemicals GmbH (Köln, Germany); AA, PGB₁, 3-phenyl-cyano(6-methoxy-2-naphthalenyl) methyl ester-2-oxiraneacetic acid (PHOME), LTC₄-d5-methyl ester, LTA₄ methyl ester, COX isoenzymes, and MK886, Cayman Chemical (Biomol, Hamburg, Germany); acetonitrile, Dulbecco's modified Eagle's high glucose medium with glutamine, geneticin, penicillin/streptomycin-solution and trypsin-EDTA, GE Healthcare Life Science (Freiburg, Germany); PGH₂, Larodan Fine Chemicals (Stockholm, SWE); Alexa Fluor 488 goat anti-rabbit, Alexa Fluor 555 goat anti-mouse, hygromycin B, Lipofectamine LTX Reagent Plus, and non-immune goat serum and Sf-900™ II SFM, Invitrogen (Darmstadt, Germany). DMSO, Merck (Darmstadt, Germany); IL-1β, ReproTech (Hamburg, Germany); ATP, Roche (Mannheim, Germany); SDS, Roth GmbH (Karlsruhe, Germany); zileuton, Sequoia Research Products (Oxford, UK); Dulbecco's Buffer Substance (PBS), SERVA Electrophoresis (Heidelberg, Germany); dithiothreitol and HPLC solvents, VWR (Darmstadt, Germany); Ca²⁺-ionophore A23187, dextrane, fetal calf serum (FCS), 3-(4,5-dimethylthiazol-2-yl)-2,5-diphenyltetrazolium bromide (MTT), non-essential amino acids, RPMI 1640 Medium, phenylmethanesulfonyl fluoride, soybean trypsin inhibitor, lysozyme, leupeptin, fatty acid free BSA, Duolink detection reagents red, Duolink PLA probe anti-rabbit PLUS, Duolink PLA probe anti-mouse MINUS, ATP agarose, Duolink wash buffers as well as other chemicals were from Sigma-Aldrich (Taufkirchen, Germany).

Cell isolation and cell culture. Peripheral blood (University Hospital Jena, Germany) was collected from fasted healthy adult donors that were informed about the aim of the study and gave written consent. The protocols for experiments with neutrophils or monocytes were approved by the ethical commission of the Friedrich-Schiller-University Jena (approval number 4292-12/14). All methods were performed in accordance with the relevant guidelines and regulations. Leukocyte concentrates were obtained by centrifugation (4000 × g, 20 min, 20 °C) of heparinized blood preparations. Neutrophils and monocytes were immediately isolated as described before⁵⁶. In brief, leukocyte concentrates were subjected to dextran sedimentation and centrifuged on lymphocyte separation medium (LSM 1077, PAA, Coelbe, Germany). For isolation of pelleted neutrophils, remaining erythrocytes were removed by hypotonic lysis, washed twice with ice-cold PBS and resuspended in medium to a cell density described for the respective experiments. Monocytes were separated from peripheral

blood mononuclear cells (PBMC) by adherence to cell culture flasks (Greiner Bio-one, Nuertingen, Germany) for 1.5 h (37 °C, 5% CO₂) in RPMI 1640 containing L-glutamine (1 mM), heat-inactivated FCS (10%), penicillin (100 U/mL) and streptomycin (100 µg/mL), followed by cell-scraping and resuspension in PBS.

HEK293 cells were cultured in monolayers (37 °C, 5% CO₂) in DMEM containing FCS (10%), penicillin (100 U/mL) and streptomycin (100 µg/mL). HEK293 cell lines stably expressing 5-LOX with or without FLAP were selected using geneticin (400 µg/mL) with or without hygromycin (200 µg/mL), respectively, as previously described²⁹. Transfection of HEK293 was performed using pcDNA3.1 plasmids and lipofectamine according to the manufacturer's instructions (Invitrogen, Darmstadt, Germany).

Sf9 cells were cultured in monolayers at 27 °C in Sf-900 II SFM medium containing FCS (10%), penicillin (100 U/mL) and streptomycin (100 µg/mL).

HepG2 cells were cultured as monolayers in RPMI 1640 containing FCS (10%), penicillin (100 U/mL) and streptomycin (100 µg/mL) at 37 °C, 5% CO₂.

Expression, purification and activity assay of human recombinant 5-LOX. Human recombinant 5-LOX was expressed in *E. coli* BL21 transformed with pT3-5-LOX plasmid at 30 °C overnight as described before⁵⁷. Cells were lysed in lysis buffer containing triethanolamine (50 mM, pH 8.0), EDTA (5 mM), phenylmethanesulfonyl fluoride (1 mM), soybean trypsin inhibitor (60 µg/mL), dithiothreitol (2 mM) and lysozyme (1 mg/mL) and homogenized by sonification (3 × 15 s). 5-LOX was purified from the 40,000 × g supernatant (20 min, 4 °C) using an ATP-agarose column and diluted with PBS buffer containing 1 mM EDTA. To determine 5-LOX product formation, aliquots (0.5 µg purified 5-LOX in 1 mL PBS plus 1 mM EDTA) were pre-incubated with the test compounds or vehicle (0.1% DMSO) on ice for 15 min and then stimulated with 20 µM AA and CaCl₂ (2 mM) for 10 min at 37 °C. The reaction was stopped with one volume of ice-cold methanol and 5-LOX products were analyzed by RP-HPLC as previously described⁵⁸. Briefly, 530 µl acidified PBS and 200 ng of internal PGB₁ standard were added and solid phase extraction using C18 RP-columns (100 mg, UCT, Bristol, PA, USA) was performed. After elution with methanol, samples were analyzed by RP-HPLC using a C-18 Radial-PAK column (Waters, Eschborn, Germany). Unless stated otherwise, 5-LOX products include all-trans-isomers of LTB₄ and 5-HpETE as well as its corresponding alcohol 5-HETE.

Determination of 5-LOX products in intact cells and corresponding homogenates. In order to examine 5-LOX product formation in intact human neutrophils and monocytes, freshly isolated cells were resuspended in PBS buffer containing 0.1% glucose and 1 mM CaCl₂ (PGC buffer) to a final cell density of 5 × 10⁶ or 2 × 10⁶, respectively. Cells were pre-incubated with the test compounds or vehicle (0.1% DMSO) at 37 °C for 15 min prior to stimulation with 2.5 µM Ca²⁺-ionophore A23187 for 10 min (37 °C) with or without supplementation of the indicated concentrations of AA. 5-LOX product formation was stopped by addition of one volume of ice-cold methanol, samples were subjected to solid phase extraction after addition of 200 ng PGB₁ as internal standard and 5-LOX products were analyzed by RP-HPLC as described above.

Determination of 5-LOX products in corresponding homogenates was performed by resuspending neutrophils (final density of 5 × 10⁶ cells/mL) or monocytes (2 × 10⁶ cells/mL) in PBS containing 1 mM EDTA and sonicated on ice (3 × 15 s). Aliquots of homogenates were pre-incubated with the test compounds or vehicle (0.1% DMSO) on ice for 15 min and stimulated with 20 µM AA and CaCl₂ (2 mM) at 37 °C for 10 min. 5-LOX product formation was assayed as described for intact cells above.

For analysis of 5-LOX product formation in HEK293 cells stably expressing 5-LOX with or without FLAP, cells were harvested by trypsinization, pelleted (1,200 rpm, 5 min, 4 °C) and resuspended in PGC buffer to a final concentration of 1 × 10⁶ cells/mL. Aliquots were pre-incubated with test compounds or 0.1% DMSO for 15 min, respectively, and stimulated with 2.5 µM A23187 and 3 µM AA. After termination of the incubations by addition of one volume of ice-cold methanol, samples were subjected to solid phase extraction and analysis of 5-LOX products as described above.

Determination of LTA₄ hydrolase activity. In order to determine the activity of LTA₄-H, aliquots of human recombinant 5-LOX (0.5 µg) and 10 µg of human recombinant LTA₄-H (kindly provided by Dr. E. Proschak, Goethe University, Frankfurt, Germany) were suspended in 1 mL PBS containing 1 mM EDTA and pre-incubated with test compounds or vehicle (0.1% DMSO) for 10 min on ice. The specific LTA₄-H inhibitor SC57461A (0.3 µM) was used as reference drug. Subsequently, incubations were stimulated with 20 µM AA and 2 mM CaCl₂ for additional 10 min at 37 °C. The reaction was stopped by 1 volume ice-cold methanol, 530 µL acidified PBS and 200 ng of PGB₁ as internal standard were added and subjected to solid phase extraction. All LTB₄ isomers were analyzed by HPLC as described above.

Expression, purification and activity assays of human recombinant sEH. Human recombinant sEH was expressed and purified as reported before⁵⁹. In brief, Sf9 cells were infected with a recombinant baculovirus (kindly provided by Dr. B. Hammock, University of California, Davis, CA). 72 hrs post-transfection, cells were pelleted and sonicated (3 × 10 sec at 4 °C) in lysis buffer containing NaHPO₄ (50 mM, pH 8), NaCl (300 mM), glycerol (10%), EDTA (1 mM), phenylmethanesulfonyl fluoride (1 mM), leupeptin (10 µg/mL), and soybean trypsin inhibitor (60 µg/mL). Supernatants after centrifugation at 100,000 × g (60 min, 4 °C) were subjected to a benzylthio-sepharose-affinity chromatography in order to purify sEH by elution with 4-fluorochalcone oxide in PBS containing DTT (1 mM) and EDTA (1 mM). Dialyzed and concentrated (Millipore Amicon-Ultra-15 centrifugal filter) enzyme solution was assayed for total protein with Bio-Rad protein detection kit (Bio-Rad Laboratories, Munich, Germany) and the epoxide hydrolase activity was determined by using a fluorescence-based assay as described before⁶⁰. Briefly, sEH was diluted in Tris buffer (25 mM, pH 7) supplemented with BSA (0.1 mg/mL) to an appropriate enzyme concentration and pre-incubated with test compounds

or vehicle (0.1% DMSO) for 10 min at room temperature (RT). The reaction was started by addition of 50 μM 3-phenyl-cyano(6-methoxy-2-naphthalenyl)methyl ester-2-oxiraneacetic acid (PHOME), a non-fluorescent compound that is enzymatically converted into fluorescent 6-methoxy-naphthaldehyde at RT. After 60 min, reactions were stopped by ZnSO_4 (200 mM) and fluorescence was detected (λ_{em} 465 nm, λ_{ex} 330 nm) and potential fluorescence of test compounds was subtracted from the read-out, if required.

In order to analyze the phosphatase activity of sEH, a recently published assay⁶¹ was performed. In brief, purified sEH-phosphatase-domain was pre-incubated with test compounds or vehicle (0.1% DMSO), in acetate buffer (50 mM, pH 5.8) containing MgCl_2 (10 mM) and Triton-X-100 (0.01%) for 30 min at RT prior to addition of 6,8-difluoro-4-methylumbelliferyl phosphate (DiFMUP, 300 μM). Phosphatase activity was assayed by measurement of fluorescence (λ_{ex} 360 nm, λ_{em} 450 nm) of the dephosphorylated DiFMU for 45 min at 37 °C.

Determination of 14,15-DiHETrE-formation in HepG2 cells and in a cell-free assay. To assay the activity of sEH in a cell-based model, HepG2 cells were harvested by trypsinization, pelleted (1,200 rpm, 5 min, 4 °C) and resuspended in PGC buffer to a final concentration of 1.5×10^6 cells/mL. Cells were pre-incubated with test compounds or 0.1% DMSO at 37 °C for 15 min, and incubated with 1.5 μM 14,15-EET (Cayman Chemical, Biomol, Hamburg, Germany) for 30 min at 37 °C. After termination of the reactions with one volume of ice-cold methanol, 1.31 ng d8-5(S)-HETE and 1.36 ng d4-LTB₄ (Cayman Chemical, Biomol, Hamburg, Germany) were added as internal standards and samples were subjected to solid phase extraction. Briefly, samples were acidified with four volumes of MilliQ water pH 3.5 containing PBS-HCl and subjected to Waters Sep-Pak[®] Vac 6cc columns (Waters, Milford, MA, USA), washed once with MilliQ and hexane, and eluted with methylformiate. The nitrogen-dried samples were dissolved in 50% methanol, and 14,15-DiHETrE formation was measured by UPLC-MS/MS using an Acquity[™] UPLC system (Waters, Milford, MA, USA) and a QTRAP 5500 Mass Spectrometer (ABSciex, Darmstadt, Germany) equipped with a Turbo V[™] Source and electrospray ionization (ESI). In brief, lipid mediators were separated using a Sep-Pak C18 35 cc Vac Cartridge, 10 g Sorbent per Cartridge, 55–105 μm Particle Size, 10/pk (Waters, Milford, MA, USA) at 50 °C with a flow rate of 0.3 mL/min. MilliQ water (A) and methanol (B) both acidified with 0.1% acetic acid were used as solvents with an increasing percentage of B starting at 42% and ending with 86% at 12.5 min followed by isocratic elution at 98% B for another 3 min. Analytes were detected by multiple reaction monitoring in the negative ion mode using the following transitions: 14,15-EET (m/z 319 \rightarrow 219), 14,15-DiHETrE (m/z 337 \rightarrow 207), d8-5(S)-HETE (m/z 327 \rightarrow 116) and d4-LTB₄ (m/z 339 \rightarrow 197). Ion spray voltage was set to 4000 V, the heater temperature to 500 °C, the declustering potential to 50–80 eV, the entrance potential to 10 eV, the collision cell exit potential to 10–13 eV, collision energies of 10 eV, the spray gas pressure to 40 psi, medium collision gas and the curtain gas pressure to 35 psi.

In order to confirm the identity of detected metabolites, human recombinant sEH was diluted in 25 mM Tris buffer pH 7.0 to a final concentration of 0.3 $\mu\text{g}/\text{mL}$ and pre-incubated with test compounds or 0.1% DMSO on ice for 15 min and stimulated with 14,15-EET (1.5 μM , 30 min, 37 °C). Extraction and detection of metabolites was performed as described for the cell-based assay.

Determination of microsomal PGE₂ synthase activity. To perform the analysis of microsomal PGE₂ synthase (mPGES)-1 activity, microsomal preparations of A549 cells were obtained as described before⁶². Briefly, A549 cells were cultivated in DMEM medium containing FCS (2%) and IL-1 β (2 ng/mL) for 72 h (37 °C, 5% CO₂). Cells were harvested and resuspended in homogenization buffer consisting of potassium phosphate (0.1 M, pH 7.4), phenylmethanesulfonyl fluoride (1 mM), soybean trypsin inhibitor (60 $\mu\text{g}/\text{mL}$), leupeptin (1 $\mu\text{g}/\text{mL}$), glutathione (2.5 mM), and sucrose (250 mM). After freezing the cells in liquid nitrogen and sonication (3 \times 20 s), a differential centrifugation at 10,000 g (10 min, 4 °C) and 174,000 \times g (60 min, 4 °C) was performed and pellets were resuspended in homogenization buffer. To assay mPGES-1 activity, microsomes were diluted in potassium phosphate buffer (0.1 M, pH 7.4) with glutathione (2 mM) and pre-incubated with the test compounds or vehicle (0.1% DMSO) on ice for 15 min. After stimulation (1 min, 4 °C) with 20 μM PGH₂ the reaction was terminated by addition of stop solution containing FeCl_3 (40 mM), citric acid (80 mM), and 11 β -PGE₂ (10 μM as internal standard) and analyzed for PGE₂ product formation by RP-HPLC as reported before⁶².

Determination of LTC₄ synthase (LTC₄S) activity. LTC₄S activity was assayed by using microsomes of HEK293 cells stably expressing LTC₄S, as previously published⁶³. In brief, HEK293 expressing LTC₄S were cultivated as described above and selected using geneticin (400 $\mu\text{g}/\text{mL}$). Isolation of microsomes was performed as described for mPGES-1 above and microsomes were diluted in potassium phosphate buffer (0.1 M, pH 7.4) with glutathione (5 mM) to a final concentration of 2.5 μg protein per mL. After pre-incubation with the test compounds or vehicle (2% DMSO) for 10 min at 4 °C, reactions were started by addition of 1 μM LTA₄-methyl ester and stopped by addition of one volume of ice-cold methanol after 10 min of incubation at 4 °C. To determine enzyme activity, acidified PBS and d₅-LTC₄-methyl ester (5 ng) as internal standard were added prior solid phase extraction and LTC₄-methyl ester formation was analyzed by UPLC-MS/MS as described⁶³.

Determination of COX activity. COX activity was assayed by using purified ovine COX-1 and recombinant human COX-2, respectively. Enzymes were diluted in Tris buffer (100 mM, pH 8) supplemented with glutathione (5 mM), EDTA (100 μM) and hemoglobin (5 μM) to a final concentration of 50 U/mL (COX-1) or 20 U/mL (COX-2) and pre-incubated with test compounds or vehicle (0.1% DMSO) for 5 min at RT. After 30 sec at 37 °C, reactions were started with 5 μM AA (COX-1) or 2 μM AA (COX-2) and stopped after 5 min at 37 °C by addition of one volume of ice-cold methanol. Solid phase extraction was performed as described above after addition of 200 ng of internal PGB₁ standard and COX product formation was determined by analysis of 12-HHT formation as reported before⁶⁴.

Analysis of acute cytotoxicity. Acute cytotoxicity of the compounds was determined using freshly isolated monocytes. Cells (0.2×10^6) per sample were seeded in 100 μ L buffer on 96-well plates and treated with the test compounds and appropriate controls for 24 or 48 hrs (37 °C, 5% CO₂). After addition of MTT (5 mg/mL) for 2 h (37 °C, 5% CO₂), cells were lysed by SDS treatment (10%, pH 4.5) for 16–20 hrs and formazan formation was determined by measurement of absorbance at 570 nm.

Determination of [³H]-labeled arachidonic acid release. Freshly isolated human neutrophils were resuspended in RPMI 1640 medium to a final cell density of 10^7 cells/mL and incubated with 0.5 μ Ci/mL of [³H]-labeled arachidonic acid ([³H]-AA), corresponding to a concentration of 5 nM of the fatty acid, for 2 hrs (37 °C, 5% CO₂). Cells were washed twice to remove unincorporated [³H]-AA and resuspended in PBS containing glucose (0.1%), fatty acid-free BSA (2 mg/mL) and CaCl₂ (1 mM). Aliquots of 10^7 cells were pre-incubated with the test compounds or vehicle (0.1% DMSO) at 37 °C for 10 min and stimulated with 2.5 μ M A23187 for another 10 min. The reaction was stopped on ice and cells were centrifuged at 1,200 rpm (10 min, 4 °C). The collected supernatants were combined with 2 mL of liquid scintillation counting solution (Rotiszint eco plus, Carl Roth, Karlsruhe, Germany) and assayed for radioactivity by scintillation counting (Micro Beta Trilux, Perkin Elmer, Waltham, MA).

Immunofluorescence microscopy (IF) and proximity ligation assay (PLA). In order to investigate cellular redistribution of 5-LOX and FLAP in monocytes, freshly isolated PBMC were seeded onto glass coverslips in RPMI 1640 containing L-glutamine (1 mM), heat-inactivated FCS (10%), penicillin (100 U/mL) and streptomycin (100 μ g/mL) for 1.5 hrs (37 °C, 5% CO₂). Cells were washed twice with PBS and pre-incubated with test compounds or vehicle control (0.1% DMSO) in PGC buffer for 15 min (37 °C) prior to stimulation with A23187 (2.5 μ M, 10 min, 37 °C). The incubations were stopped by paraformaldehyde fixation (4%, 20 min, RT) and cells were permeabilized using 100% ice-cold acetone (5 min, 4 °C). Blocking with non-immune goat serum (30 min, RT) was performed prior to overnight incubation (4 °C) with primary monoclonal-mouse-anti-5-LOX antibody (1:100 dilution, a generous gift from Dr. D. Steinhilber, Goethe University Frankfurt, Germany) and polyclonal-rabbit-anti-FLAP antibody (5 μ g/mL, Abcam, Cambridge, UK). Incubation with fluorophore-labeled secondary Alexa Fluor 488 goat anti-rabbit (1:1000) and Alexa Fluor 555 goat anti-mouse (1:1000) was processed for 30 min in the dark at RT and nuclear DNA was stained with DAPI-containing ProLong diamond antifade mountant (Invitrogen, Darmstadt, Germany) on glass slides. Cells were visualized by a Zeiss Axiovert 200 M microscope, and a Plan Neofluar \times 100/1.30 Oil (DIC III) objective (Carl Zeiss, Jena, Germany) and image acquisition was performed using an AxioCam MR camera (Carl Zeiss).

In situ protein interaction of 5-LOX and FLAP was analyzed by proximity ligation assay as described before³⁷ and referring to the manufacturer's protocol⁶⁵. In brief, freshly isolated monocytes were treated as described for IF above. Overnight incubations with primary antibodies were then treated for 1 h (37 °C) with oligonucleotide-labeled specific secondary antibodies (PLA probes anti-mouse MINUS and anti-rabbit PLUS). Formation of circled DNA sequences was induced by addition of ligase and oligonucleotide mixture (30 min at 37 °C). Rolling-circle-amplification of newly generated DNA template was performed (90 min, 37 °C) including hybridization of fluorescently-labeled oligonucleotides within the formed DNA strands, resulting in visualization of protein-protein interactions recognized as magenta-stained dots. Nuclear DNA staining with DAPI and image acquisition was performed as described above. Overview images were obtained using a Plan Neofluar 40/1.30 Oil (DIC III) objective (Carl Zeiss).

Murine peritonitis model. The animal studies are reported in accordance with the ARRIVE guidelines for reporting animal research⁶⁶. Male CD-1 mice (33–39 g, 8–9 weeks, Charles River Laboratories, Calco, Italy) were housed in a controlled environment (21 ± 2 °C) and provided with standard rodent chow and water ad libitum. Mice received a standard diet containing 5.7% fat, 18.9% protein and 57.3% carbohydrate (Global Diet 2018, ENVIGO, Italy). The fatty acid composition was according to Matias *et al.*⁶⁷.

Prior to experiments, all mice were allowed to acclimate for 5 days and kept at 12 h light–dark schedule, in which experiments were performed during the light phase. Animal care was in compliance with Italian regulations on protection of animals used for experimental and other scientific purpose (Ministerial Decree 116/92) and with the European Economic Community regulations (Official Journal of E.C. L 358/1 12/18/1986). Animal studies were approved by the local ethical committee of the University of Naples Federico II on 27 February 2014 (approval number 2014/18760). Mice were treated with diflupolol (1, 3 or 10 mg/kg), MK886 (1 or 3 mg/kg), zileuton (10 mg/kg) or vehicle (0.9% saline solution containing 2% DMSO), received as intraperitoneal (i.p.) injection, 30 min prior induction of peritonitis according to well-recognized experimental design for studying LT synthesis inhibitors in acute inflammation²⁷. Zymosan (Sigma, Milan, Italy) was prepared and injected i.p. as a final suspension (2 mg/mL) in 0.9% saline solution after boiling, centrifugation and sonication. Peritoneal lavage (3 mL of cold PBS) was performed after CO₂-euthanasia at indicated time points, followed by 60 sec of gentle manual massage. Two mL of exudates were collected and infiltrated cells were determined using a Burker chamber and vital trypan blue staining. Pelleted samples (18,000 \times g, 5 min, 4 °C) were frozen (–80 °C) and assayed for myeloperoxidase (MPO) activity (pellet) or LTC₄ and LTB₄ formation (supernatant), respectively.

MPO of neutrophils was examined as follows: pellets from exudates were resuspended in PBS (50 mM, pH 6) containing 0.5% hexadecyltrimethyl-ammonium bromide and sonicated, followed by 3 freeze–thawing cycles and a final sonication. Supernatants of centrifuged samples (18,000 \times g, 30 min) were added to a 96-well plate and reactions were initiated by addition of PBS (50 mM, pH 6) containing o-dianisidine (0.167 mg/mL) and hydrogen peroxide (0.0005%). Absorbance was monitored in the kinetic mode (Biorad Imark microplate) and levels of MPO were determined using a calibration curve with human neutrophils as reference standard. MPO levels were

expressed as units MPO per mouse. LTC₄ and LTB₄ formation within the supernatants were determined by EIA (Enzo Life Sciences International Inc., Lörrach, Germany) according to manufacturer's protocol³⁹.

Vascular permeability was assessed according to a previous report²⁷. Briefly, 0.3 mL of 0.9% saline solution supplemented with Evans blue dye (40 mg/kg) was injected intravenously (i.v.) into the caudal vein followed by immediate peritonitis induction (using zymosan). After 30 min, peritoneal lavage exudates of CO₂-euthanized were collected as described above. Absorbance of the centrifuged supernatants (3,000 × g, 5 min) was measured at 650 nm (Beckman Coulter DU730).

Statistics. Results are presented as mean ± standard error of the mean out of *n* independent experiments, where *n* represents the number of performed experiments on different days or with different donors or the number of animals for *in vivo* studies. IC₅₀ values were calculated from at least 5 different concentrations using a nonlinear regression interpolation of semi-logarithmic graphs in GraphPad Prism (GraphPad Software Inc., San Diego, CA). Statistical evaluation was performed by one-way ANOVA using GraphPad InStat (GraphPad Software Inc., San Diego, CA) followed by a Bonferroni post-hoc test for multiple or student t-test for single comparisons, respectively. P-values < 0.05 were considered as significant.

References

- Harizi, H., Corcuff, J. B. & Gualde, N. Arachidonic-acid-derived eicosanoids: roles in biology and immunopathology. *Trends Mol Med* **14**, 461–469, doi:10.1016/j.molmed.2008.08.005 (2008).
- Haeggstrom, J. Z. & Funk, C. D. Lipoxygenase and leukotriene pathways: biochemistry, biology, and roles in disease. *Chem. Rev.* **111**, 5866–5898, doi:10.1021/cr200246d (2011).
- Capdevila, J. *et al.* The oxidative metabolism of arachidonic acid by purified cytochromes P-450. *Biochem. Biophys. Res. Commun.* **101**, 1357–1363 (1981).
- Spector, A. A., Fang, X., Snyder, G. D. & Weintraub, N. L. Epoxyeicosatrienoic acids (EETs): metabolism and biochemical function. *Prog. Lipid Res.* **43**, 55–90 (2004).
- Rao, P. & Knaus, E. E. Evolution of nonsteroidal anti-inflammatory drugs (NSAIDs): cyclooxygenase (COX) inhibition and beyond. *J. Pharm. Pharm. Sci.* **11**, 81s–110s (2008).
- Steinhilber, D. & Hofmann, B. Recent advances in the search for novel 5-lipoxygenase inhibitors. *Basic Clin. Pharmacol. Toxicol.* **114**, 70–77, doi:10.1111/bcpt.12114 (2014).
- He, C. *et al.* Dynamic eicosanoid responses upon different inhibitor and combination treatments on the arachidonic acid metabolic network. *Mol. Biosyst.* **8**, 1585–1594, doi:10.1039/c2mb05503a (2012).
- Szczeklik, A., Sanak, M., Nizankowska-Mogilnicka, E. & Kielbasa, B. Aspirin intolerance and the cyclooxygenase-leukotriene pathways. *Curr. Opin. Pulm. Med.* **10**, 51–56 (2004).
- Celotti, F. & Laufer, S. Anti-inflammatory drugs: new multitarget compounds to face an old problem. The dual inhibition concept. *Pharmacol. Res.* **43**, 429–436, doi:10.1006/phrs.2000.0784 (2001).
- Morphy, R. & Rankovic, Z. Designed multiple ligands. An emerging drug discovery paradigm. *J. Med. Chem.* **48**, 6523–6543, doi:10.1021/jm058225d (2005).
- Meirer, K., Steinhilber, D. & Proschak, E. Inhibitors of the arachidonic acid cascade: interfering with multiple pathways. *Basic Clin. Pharmacol. Toxicol.* **114**, 83–91, doi:10.1111/bcpt.12134 (2014).
- Hwang, S. H. *et al.* Synthesis and structure-activity relationship studies of urea-containing pyrazoles as dual inhibitors of cyclooxygenase-2 and soluble epoxide hydrolase. *J. Med. Chem.* **54**, 3037–3050, doi:10.1021/jm2001376 (2011).
- Meirer, K. *et al.* Synthesis and structure-activity relationship studies of novel dual inhibitors of soluble epoxide hydrolase and 5-lipoxygenase. *J. Med. Chem.* **56**, 1777–1781, doi:10.1021/jm301617j (2013).
- Koeberle, A. & Werz, O. Multi-target approach for natural products in inflammation. *Drug Discov. Today* **19**, 1871–1882, doi:10.1016/j.drudis.2014.08.006 (2014).
- Temml, V. *et al.* Discovery of the first dual inhibitor of the 5-lipoxygenase-activating protein and soluble epoxide hydrolase using pharmacophore-based virtual screening. *Sci. Rep.* **7**, 42751, doi:10.1038/srep42751 (2017).
- Dixon, R. A. *et al.* Requirement of a 5-lipoxygenase-activating protein for leukotriene synthesis. *Nature* **343**, 282–284, doi:10.1038/343282a0 (1990).
- Evans, J. F., Ferguson, A. D., Mosley, R. T. & Hutchinson, J. H. What's all the FLAP about? 5-lipoxygenase-activating protein inhibitors for inflammatory diseases. *Trends Pharmacol. Sci.* **29**, 72–78, doi:10.1016/j.tips.2007.11.006 (2008).
- Gillard, J. *et al.* L-663,536 (MK-886) (3-[1-(4-chlorobenzyl)-3-t-butyl-thio-5-isopropylindol-2-yl]-2,2-dimethylpropanoic acid), a novel, orally active leukotriene biosynthesis inhibitor. *Can. J. Physiol. Pharmacol.* **67**, 456–464 (1989).
- Muller-Peddinghaus, R. *et al.* BAY X1005, a new selective inhibitor of leukotriene synthesis: pharmacology and pharmacokinetics. *J. Lipid Mediat.* **6**, 245–248 (1993).
- Morisseau, C. & Hammock, B. D. Impact of soluble epoxide hydrolase and epoxyeicosanoids on human health. *Annu. Rev. Pharmacol. Toxicol.* **53**, 37–58, doi:10.1146/annurev-pharmtox-011112-140244 (2013).
- Liu, J. Y. *et al.* Inhibition of soluble epoxide hydrolase enhances the anti-inflammatory effects of aspirin and 5-lipoxygenase activation protein inhibitor in a murine model. *Biochem. Pharmacol.* **79**, 880–887, doi:10.1016/j.bcp.2009.10.025 (2010).
- Jung, O. *et al.* Inhibition of the soluble epoxide hydrolase promotes albuminuria in mice with progressive renal disease. *PLoS One* **5**, e11979, doi:10.1371/journal.pone.0011979 (2010).
- Werz, O., Gerstmeier, J. & Garscha, U. Novel leukotriene biosynthesis inhibitors (2012–2016) as anti-inflammatory agents. *Expert Opin. Ther. Pat.* 1–14, doi:10.1080/13543776.2017.1276568 (2017).
- Menard, L., Pilote, S., Naccache, P. H., Lavolette, M. & Borgeat, P. Inhibitory effects of MK-886 on arachidonic acid metabolism in human phagocytes. *Br. J. Pharmacol.* **100**, 15–20 (1990).
- Schaible, A. M. *et al.* Elucidation of the molecular mechanism and the efficacy *in vivo* of a novel 1,4-benzoquinone that inhibits 5-lipoxygenase. *Br. J. Pharmacol.* **171**, 2399–2412, doi:10.1111/bph.12592 (2014).
- Mancini, J. A. *et al.* 5-lipoxygenase-activating protein is an arachidonate binding protein. *FEBS Lett.* **318**, 277–281 (1993).
- Garscha, U. *et al.* BRP-187: A potent inhibitor of leukotriene biosynthesis that acts through impeding the dynamic 5-lipoxygenase/5-lipoxygenase-activating protein (FLAP) complex assembly. *Biochem. Pharmacol.* **119**, 17–26, doi:10.1016/j.bcp.2016.08.023 (2016).
- Pergola, C. *et al.* The novel benzimidazole derivative BRP-7 inhibits leukotriene biosynthesis *in vitro* and *in vivo* by targeting 5-lipoxygenase-activating protein (FLAP). *Br. J. Pharmacol.* **171**, 3051–3064, doi:10.1111/bph.12625 (2014).
- Gerstmeier, J., Weinigel, C., Barz, D., Werz, O. & Garscha, U. An experimental cell-based model for studying the cell biology and molecular pharmacology of 5-lipoxygenase-activating protein in leukotriene biosynthesis. *Biochim. Biophys. Acta* **1840**, 2961–2969, doi:10.1016/j.bbagen.2014.05.016 (2014).

30. Morisseau, C. *et al.* Role of soluble epoxide hydrolase phosphatase activity in the metabolism of lysophosphatidic acids. *Biochem. Biophys. Res. Commun.* **419**, 796–800, doi:[10.1016/j.bbrc.2012.02.108](https://doi.org/10.1016/j.bbrc.2012.02.108) (2012).
31. Morisseau, C. *et al.* Structural refinement of inhibitors of urea-based soluble epoxide hydrolases. *Biochem. Pharmacol.* **63**, 1599–1608 (2002).
32. Askonas, L. J. *et al.* Pharmacological characterization of SC-57461A (3-[methyl[3-[4-(phenylmethyl)phenoxy]propyl]amino]propanoic acid HCl), a potent and selective inhibitor of leukotriene A(4) hydrolase I: *in vitro* studies. *J. Pharmacol. Exp. Ther.* **300**, 577–582 (2002).
33. Jakobsson, P. J., Morgenstern, R., Mancini, J., Ford-Hutchinson, A. & Persson, B. Membrane-associated proteins in eicosanoid and glutathione metabolism (MAPEG). A widespread protein superfamily. *Am. J. Respir. Crit. Care Med.* **161**, S20–24, doi:[10.1164/ajrccm.161.supplement_1.lta-5](https://doi.org/10.1164/ajrccm.161.supplement_1.lta-5) (2000).
34. Martinez Molina, D., Eshaghi, S. & Nordlund, P. Catalysis within the lipid bilayer-structure and mechanism of the MAPEG family of integral membrane proteins. *Curr. Opin. Struct. Biol.* **18**, 442–449, doi:[10.1016/j.sbi.2008.04.005](https://doi.org/10.1016/j.sbi.2008.04.005) (2008).
35. Lam, B. K. *et al.* Molecular cloning, expression and characterization of mouse leukotriene C4 synthase. *Eur. J. Biochem.* **238**, 606–612 (1996).
36. Claveau, D. *et al.* Microsomal prostaglandin E synthase-1 is a major terminal synthase that is selectively up-regulated during cyclooxygenase-2-dependent prostaglandin E2 production in the rat adjuvant-induced arthritis model. *J. Immunol.* **170**, 4738–4744 (2003).
37. Gerstmeier, J. *et al.* Time-resolved *in situ* assembly of the leukotriene-synthetic 5-lipoxygenase/5-lipoxygenase-activating protein complex in blood leukocytes. *FASEB J.* **30**, 276–285, doi:[10.1096/fj.15-278010](https://doi.org/10.1096/fj.15-278010) (2016).
38. Mandal, A. K. *et al.* The nuclear membrane organization of leukotriene synthesis. *Proc. Natl. Acad. Sci. USA* **105**, 20434–20439, doi:[10.1073/pnas.0808211106](https://doi.org/10.1073/pnas.0808211106) (2008).
39. Rossi, A. *et al.* *In vivo* sex differences in leukotriene biosynthesis in zymosan-induced peritonitis. *Pharmacol Res* **87**, 1–7, doi:[10.1016/j.phrs.2014.05.011](https://doi.org/10.1016/j.phrs.2014.05.011) (2014).
40. Pettersen, D., Davidsson, O. & Whatling, C. Recent advances for FLAP inhibitors. *Bioorg. Med. Chem. Lett.* **25**, 2607–2612, doi:[10.1016/j.bmcl.2015.04.090](https://doi.org/10.1016/j.bmcl.2015.04.090) (2015).
41. Miller, D. K. *et al.* Identification and isolation of a membrane protein necessary for leukotriene production. *Nature* **343**, 278–281, doi:[10.1038/343278a0](https://doi.org/10.1038/343278a0) (1990).
42. Byrum, R. S., Goulet, J. L., Griffiths, R. J. & Koller, B. H. Role of the 5-lipoxygenase-activating protein (FLAP) in murine acute inflammatory responses. *J. Exp. Med.* **185**, 1065–1075 (1997).
43. Ferguson, A. D. *et al.* Crystal structure of inhibitor-bound human 5-lipoxygenase-activating protein. *Science* **317**, 510–512, doi:[10.1126/science.1144346](https://doi.org/10.1126/science.1144346) (2007).
44. Abramovitz, M. *et al.* 5-lipoxygenase-activating protein stimulates the utilization of arachidonic acid by 5-lipoxygenase. *Eur. J. Biochem.* **215**, 105–111 (1993).
45. Fischer, L. *et al.* The molecular mechanism of the inhibition by licofelone of the biosynthesis of 5-lipoxygenase products. *Br. J. Pharmacol.* **152**, 471–480, doi:[10.1038/sj.bjp.0707416](https://doi.org/10.1038/sj.bjp.0707416) (2007).
46. Shen, H. C. & Hammock, B. D. Discovery of inhibitors of soluble epoxide hydrolase: a target with multiple potential therapeutic indications. *J. Med. Chem.* **55**, 1789–1808, doi:[10.1021/jm201468j](https://doi.org/10.1021/jm201468j) (2012).
47. Imig, J. D. Epoxides and soluble epoxide hydrolase in cardiovascular physiology. *Physiol. Rev.* **92**, 101–130, doi:[10.1152/physrev.00021.2011](https://doi.org/10.1152/physrev.00021.2011) (2012).
48. Schmelzer, K. R. *et al.* Soluble epoxide hydrolase is a therapeutic target for acute inflammation. *Proc. Natl. Acad. Sci. U S A* **102**, 9772–9777, doi:[10.1073/pnas.0503279102](https://doi.org/10.1073/pnas.0503279102) (2005).
49. Hou, H. H. *et al.* N-terminal domain of soluble epoxide hydrolase negatively regulates the VEGF-mediated activation of endothelial nitric oxide synthase. *Cardiovasc. Res.* **93**, 120–129, doi:[10.1093/cvr/cvr267](https://doi.org/10.1093/cvr/cvr267) (2012).
50. Lam, B. K., Penrose, J. F., Freeman, G. J. & Austen, K. F. Expression cloning of a cDNA for human leukotriene C4 synthase, an integral membrane protein conjugating reduced glutathione to leukotriene A4. *Proc. Natl. Acad. Sci. USA* **91**, 7663–7667 (1994).
51. Serhan, C. N. Pro-resolving lipid mediators are leads for resolution physiology. *Nature* **510**, 92–101, doi:[10.1038/nature13479](https://doi.org/10.1038/nature13479) (2014).
52. Lammerrmann, T. *et al.* Neutrophil swarms require LTB4 and integrins at sites of cell death *in vivo*. *Nature* **498**, 371–375, doi:[10.1038/nature12175](https://doi.org/10.1038/nature12175) (2013).
53. Peters-Golden, M. & Henderson, W. R. Jr. Leukotrienes. *N. Engl. J. Med.* **357**, 1841–1854, doi:[10.1056/NEJMra071371](https://doi.org/10.1056/NEJMra071371) (2007).
54. Hakonarson, H. Role of FLAP and PDE4D in myocardial infarction and stroke: target discovery and future treatment options. *Curr. Treat Options Cardiovasc. Med.* **8**, 183–192 (2006).
55. Hwang, S. H., Weckler, A. T., Wagner, K. & Hammock, B. D. Rationally designed multitarget agents against inflammation and pain. *Curr. Med. Chem.* **20**, 1783–1799 (2013).
56. Boyum, A. Isolation of mononuclear cells and granulocytes from human blood. Isolation of mononuclear cells by one centrifugation, and of granulocytes by combining centrifugation and sedimentation at 1 g. *Scand. J. Clin. Lab. Invest. Suppl* **97**, 77–89 (1968).
57. Fischer, L., Szellas, D., Radmark, O., Steinhilber, D. & Werz, O. Phosphorylation- and stimulus-dependent inhibition of cellular 5-lipoxygenase activity by nonredox-type inhibitors. *FASEB J.* **17**, 949–951, doi:[10.1096/fj.02-0815fje](https://doi.org/10.1096/fj.02-0815fje) (2003).
58. Steinhilber, D., Herrmann, T. & Roth, H. J. Separation of lipoxins and leukotrienes from human granulocytes by high-performance liquid chromatography with a Radial-Pak cartridge after extraction with an octadecyl reversed-phase column. *J. Chromatogr.* **493**, 361–366 (1989).
59. Wixtrom, R. N., Silva, M. H. & Hammock, B. D. Affinity purification of cytosolic epoxide hydrolase using derivatized epoxy-activated Sepharose gels. *Anal. Biochem.* **169**, 71–80 (1988).
60. Waltenberger, B. *et al.* Discovery of Potent Soluble Epoxide Hydrolase (sEH) Inhibitors by Pharmacophore-Based Virtual Screening. *J. Chem. Inf. Model* **56**, 747–762, doi:[10.1021/acs.jcim.5b00592](https://doi.org/10.1021/acs.jcim.5b00592) (2016).
61. Klingler, F. M., Wolf, M., Wittmann, S., Gribbon, P. & Proschak, E. Bacterial Expression and HTS Assessment of Soluble Epoxide Hydrolase Phosphatase. *J. Biomol. Screen.* **21**, 689–694, doi:[10.1177/1087057116637609](https://doi.org/10.1177/1087057116637609) (2016).
62. Koeberle, A. *et al.* Licofelone suppresses prostaglandin E2 formation by interference with the inducible microsomal prostaglandin E2 synthase-1. *J. Pharmacol. Exp. Ther.* **326**, 975–982, doi:[10.1124/jpet.108.139444](https://doi.org/10.1124/jpet.108.139444) (2008).
63. Liening, S. *et al.* Development of smart cell-free and cell-based assay systems for investigation of leukotriene C4 synthase activity and evaluation of inhibitors. *Biochim. Biophys. Acta.* **1861**, 1605–1613, doi:[10.1016/j.bbailip.2016.07.011](https://doi.org/10.1016/j.bbailip.2016.07.011) (2016).
64. Albert, D. *et al.* Hyperforin is a dual inhibitor of cyclooxygenase-1 and 5-lipoxygenase. *Biochem. Pharmacol.* **64**, 1767–1775 (2002).
65. Soderberg, O. *et al.* Direct observation of individual endogenous protein complexes *in situ* by proximity ligation. *Nat. Methods* **3**, 995–1000, doi:[10.1038/nmeth947](https://doi.org/10.1038/nmeth947) (2006).
66. Kilkenny, C., Browne, W. J., Cuthill, I. C., Emerson, M. & Altman, D. G. Improving bioscience research reporting: the ARRIVE guidelines for reporting animal research. *PLoS Biol.* **8**, e1000412, doi:[10.1371/journal.pbio.1000412](https://doi.org/10.1371/journal.pbio.1000412) (2010).
67. Matias, I. *et al.* Dysregulation of peripheral endocannabinoid levels in hyperglycemia and obesity: Effect of high fat diets. *Mol. Cell. Endocrinol.* **286**, S66–78, doi:[10.1016/j.mce.2008.01.026](https://doi.org/10.1016/j.mce.2008.01.026) (2008).

Acknowledgements

D.S. is an Ingeborg Hochmair Professor of the University of Innsbruck. S.K. received a doctoral fellowship by the Excellence Graduate School Jena School for Microbial Communication (JSMC). This work was supported by the Deutsche Forschungsgemeinschaft, SFB 1127 (“ChemBioSys”) and GA 2101/2-1.

Author Contributions

U.G., E.R., and O.W. designed research; E.R., S.P., A.R., V.T., D.S., S.K., J.G., S.L., H.A., S.W., M.W., C.W., S.R., G.K.S. performed research; U.G., E.R., L.S., D.S., and O.W. analyzed data; and U.G., E.R. and O.W. wrote the paper.

Additional Information

Competing Interests: The authors declare that they have no competing interests.

Publisher's note: Springer Nature remains neutral with regard to jurisdictional claims in published maps and institutional affiliations.



Open Access This article is licensed under a Creative Commons Attribution 4.0 International License, which permits use, sharing, adaptation, distribution and reproduction in any medium or format, as long as you give appropriate credit to the original author(s) and the source, provide a link to the Creative Commons license, and indicate if changes were made. The images or other third party material in this article are included in the article's Creative Commons license, unless indicated otherwise in a credit line to the material. If material is not included in the article's Creative Commons license and your intended use is not permitted by statutory regulation or exceeds the permitted use, you will need to obtain permission directly from the copyright holder. To view a copy of this license, visit <http://creativecommons.org/licenses/by/4.0/>.

© The Author(s) 2017